

**EFFECTS OF FUNCTIONALIZED ZnO NANOPARTICLES ON THE  
PHYTOHORMONES: GROWTH AND DEVELOPMENT OF *SOLANUM  
MELONGENA* L. (BRINJAL) PLANT**

**Sharda Sundaram Sanjay<sup>1\*</sup>, Avinash C. Pandey<sup>2</sup>, Madhulika Singh<sup>3</sup>, Sheo M. Prasad<sup>3</sup>**

<sup>1</sup> Department of Chemistry, Ewing Christian College, Allahabad-211002

<sup>2</sup> Nanotechnology Application Centre, University of Allahabad, Allahabad-211002

<sup>3</sup> Ranjan Plant Physiology and Biochemistry Laboratory, Department of Botany, University of Allahabad, Allahabad-21102, India.

Article Received on  
21 Feb 2015,

Revised on 12 March 2015,  
Accepted on 03 April 2015

**\*Correspondence for**

**Author**

**Sharda Sundaram**

**Sanjay**

Department of Chemistry,  
Ewing Christian College,  
Allahabad-211002

**ABSTRACT**

In this paper functionalized ZnO nanoparticles were synthesized through *in situ* functionalization method and characterized it by XRD, SEM and FTIR spectroscopy. The functionalized ZnO nanoparticles were then applied to the *Solanum melongena* i.e. brinjal (var. Rajni) plant to investigate its effect on the activity of phytohormones by measuring plant growth and development, photosynthetic pigment in leaves and total soluble proteins. The potent antioxidant activity of functionalized nano ZnO was also determined by determining the level of superoxide radical and hydrogen peroxide, lipid peroxidation, total phenolics, DPPH assay, SOD, POD and GST activities. It was found that only at particular concentration nano ZnO (50 mg/L) showed its positive response to the plant and at higher concentration of nanoparticles and bulk ZnO (50 mg/L and 100 mg/L) showed phytotoxic activity.

**KEY WORDS:** Antioxidants, functionalization, lipid peroxidation, nanoparticles, phytohormones,

**INTRODUCTION**

It is an era of the advancement in the field of chemical synthesis and nanoparticles play vital role in this field. It is due to this reason, it has extensive applications in different fields, ranging from optoelectronic to catalytic functions and from bio-imaging to bio-

technology.<sup>[1-5]</sup> The use of nanoparticles in technological applications becomes limited sometimes because of its restricted behavior in different solvents. Molecular engineering on the surfaces of nanoparticles making possible to certain extent in tuning their properties to explore and develop their applicatory uses in the field of nanotechnology.<sup>[6]</sup> Nanoparticles are viable to biomedical applications, since molecular or cellular parts are much smaller and in the submicron size domain ranging from 2nm–100  $\mu$ m (a cell (10–100  $\mu$ m), a protein (5–50 nm), a gene (2 nm wide and 10–100 nm length). This means that they can easily be matched to a biological entity of interest. This simple size suggests the idea of using nanoparticles as very small probes that would allow us to spy at the cellular machinery without introducing too much interference. Chemical modifications of the nanoparticles surface are therefore necessary for specific interactions with biomolecules of interest. This goal can be achieved by controlling the surface chemical composition through functionalization and mastering its modification at the nanometer scale which offers high-added value applications to these nanoparticles. Surface functionalization means the introduction of chemical entities or functional groups on the surface of the nanoparticles, which creates specific surface sites. By controlling the nanoparticle surfaces one can tailor the particle size<sup>[7]</sup> and solubility.<sup>[8]</sup> Mainly two methods of surface modification of nanoparticles are in practice, firstly by Post – functionalization, which is done by the grafting of organic groups onto the surface of nanomaterials after the synthesis<sup>[9]</sup> and secondly, *In situ* functionalization, where the surface modification of nanomaterials is done by organic compounds during synthetic process.<sup>[10,11]</sup>

In the present paper we have synthesized functionalized ZnO nanoparticles through *in situ* functionalization method and characterized it by XRD, SEM and FTIR spectroscopy. The functionalized ZnO nanoparticles were then applied to the *Solanum melongena* i.e. brinjal (var. Rajni) plant to investigate its effect on the activity of phytohormones by measuring plant growth and development, photosynthetic pigment in leaves and total soluble proteins. Phytohormones are not nutrients but they are chemicals present at extremely low concentrations which promote, influence the growth and regulate the cellular processes.<sup>[12]</sup> The potent antioxidant activity of functionalized nano ZnO were also determined by determining the level of superoxide radical and hydrogen peroxide, lipid peroxidation, total phenolics, DPPH assay, SOD, POD and GST activities.

## Experimental

### Chemicals

The zinc acetate dihydrate ( $\text{Zn}(\text{CH}_3\text{COOH})_2 \cdot 2\text{H}_2\text{O}$ ) (99% purity), Sodium hydroxide (NaOH) (98.5% purity), Ethylene glycol (EG) (99% purity), Ethyl Alcohol (EtOH) (99% purity), sodium hypochlorite, potassium phosphate, acetone, hydroxylamine, sulfanilamide, naphthylethylene diamine dihydrochloride, diethyl ether, trichloro acetic acid (TCA), thiobarbituric acid (TBA), riboflavin, EDTA, methionine, nitro blue tetrazolium (NBT), sodium carbonate, pyrogallol,  $\text{H}_2\text{O}_2$ , 1-chloro-2,4-dinitrobenzene (CDNB), glutathione (GSH), guaiacol, acetonitrile, Indole acetic acid. All reagents were purchased from E. Merck Limited, Mumbai-400018, India. These chemicals were directly used without any special treatment.

### Preparation of ZnO nanoparticles

ZnO nanoparticles were synthesized by co-precipitation method. An aqueous solution of 0.1 M  $\text{Zn}(\text{CH}_3\text{COOH})_2 \cdot 2\text{H}_2\text{O}$  and 0.1M NaOH were prepared by dissolving each salt in a binary solvent mixture of 50-50% ethylene glycol and double distilled water. Both the solutions of  $\text{Zn}(\text{CH}_3\text{COOH})_2 \cdot 2\text{H}_2\text{O}$  and NaOH were then mixed together and placed on magnetic stirrer for stirring at  $60^\circ\text{C}$  for 4h. The resulting white solid products were collected after centrifugation and washed with double distilled water and ethanol.

### Instrumentation

The crystal structure of functionalized ZnO nanoparticles were characterized by X-ray diffraction (XRD, Rigaku D/MAX- 2200H/PC,  $\text{Cu K}\alpha$  radiation). The scanning electron microscopy (SEM) images were taken on a LEO Electron Microscopy Ltd, England. The absorbance of leaf extract was read at 663.2, 646.5 and 470 nm by using UV- visible spectrophotometer (Model 1700, Shimadzu, Japan). FT-infra red spectrum was recorded on ABB Bommen IR spectrometer (model FTLA 2000). HPLC analysis were performed on Metrohm HPLC consisting of 820 IC separation centre, 830 IC interface and twin 818 IC pump.

### Plant Material, Treatment and Plant Growth Conditions

The seeds of *Solanum melongena* i.e. brinjal were purchased from certified supplier from Rajani Seeds Pvt.Ltd., Nagpur, India. The healthy seeds were surface sterilized in 10% (v/v) sodium hypochlorite solution for 15 min. followed by repeated thorough washing with sterilized distilled water and soaked for 2 - 4 h in distilled water. After this, the uniform sized

seeds were sown in plastic trays containing sterilized sand and kept in darkness for seed germination at  $25 \pm 2^\circ\text{C}$ . The seedlings were placed in growth chamber (CDR model GRW-300 DGe, Athens) under photosynthetically active radiation (PAR) of  $150 \text{ mmol photons m}^{-2} \text{ s}^{-1}$  with 16:8 h day- night regime and 65-70% relative humidity at  $25 \pm 2^\circ\text{C}$  for a period until the secondary leaves emerged. Uniformed sized seedlings of *Solanum melongena* having secondary leaves were randomly selected and used to analyze the impact of ZnO nano and ZnO bulk on various physiological and biochemical parameters. After 15th day of seed germination seedlings were treated with 50 and 100  $\text{mg L}^{-1}$  of ZnO nano and bulk in hydroponics system.

#### ***Bulk and nano ZnO treatments***

The uniform sized seedlings having secondary leaves were gently up rooted from sand and their roots were washed gently in tap water. Thereafter, seedlings were acclimatized in half strength Hoagland's nutrient solution for 24 h. After this, experimental set up was made with 5 combinations: i) controlled (C: without treatment), ii) seedlings treated with ZnO bulk ( $B_1: 50 \text{ mg L}^{-1}$ ), iii) with ZnO bulk ( $B_2: 100 \text{ mg L}^{-1}$ ), iv) with ZnO nano ( $N_1: 50 \text{ mg L}^{-1}$ ) and v) with ZnO nano ( $N_2: 100 \text{ mg L}^{-1}$ ). The ZnO bulk and ZnO nano concentrations ( $B_1$ ,  $B_2$ ,  $N_1$  and  $N_2$ ) that have been used in the present study were environmentally relevant based on earlier studies. After the treatment all the seedlings were again placed in growth chamber for 7 days under  $150 \text{ mmol photons m}^{-2} \text{ s}^{-1}$  of PAR with 16:8 h day- night regime and at the same above mentioned conditions. During this period, medium was changed twice and aerated daily to avoid root anoxia. After 7 days of treatment, the seedlings were harvested and various parameters were analyzed immediately.

#### ***Determination of growth and photosynthetic pigments***

The growth was measured in terms of plant fresh weight. Three seedlings were selected randomly from control and treated samples, divided into root and shoot and then their fresh mass were determined. The 20 mg fresh leaves from each sample were crushed in 80% acetone and the pigments were extracted and centrifuged. The amount of chlorophyll *a*, chlorophyll *b* and carotenoids was calculated with the help of the absorbance of extract recorded at 663.2, 646.5 and 470 nm.<sup>[13]</sup>

#### ***Total soluble proteins***

Fresh leaf material (50 mg) was crushed with 1 ml of 50 mM potassium phosphate buffer [ $\text{K}_2\text{HPO}_4$  (Mol. wt. 174.18) +  $\text{KH}_2\text{PO}_4$  (Mol. wt. 136.09)] in an ice bath. The aliquot was

centrifuged at 10,000 x g for 15 min at 4 °C. Protein contents of the extract were determined following Bradford method<sup>[14]</sup> The absorbance of the colored aqueous phase was recorded at 595 nm.

#### ***Determination of Indole acetic acid***

The level of indole acetic acid (IAA) was checked with the help of HPLC analysis. Water with conductivity lower than 0.05 mS/cm and acetonitrile were of HPLC grade. The standard solution (1000 ppm) of IAA was prepared by dissolving it in the HPLC mobile phase. The mobile phase was 20% acetonitrile/water containing 1% acetic acid at a flow rate of 1 ml/min. Ten-microlitre samples of C, B<sub>1</sub>, B<sub>2</sub>, N<sub>1</sub> and N<sub>2</sub> were injected one by one after running the column with standard and then their chromatograms were recorded (fig.6).

#### ***Determination of superoxide radical and hydrogen peroxide***

Superoxide radical (SOR; O<sub>2</sub><sup>•-</sup>) in each sample was determined by Elstner and Heupel's method.<sup>[15]</sup> This assay is based on the formation of NO<sub>2</sub><sup>-</sup> from hydroxylamine in the presence of O<sub>2</sub><sup>•-</sup>. Fresh leaves and root (100 mg) were crushed in 2 ml of 65 mM potassium phosphate buffer (pH 7.8) and centrifuged at 10,000g for 10 min at 4°C (CPR-30, Remi, India). The reaction mixture consisted of 65 mM potassium phosphate buffer (pH 7.8), 10 mM hydroxylamine hydrochloride and tissue extract were incubated for 20 min at 25°C. After this, 17 mM sulfanilamide and 7 mM naphthylethylene diamine dihydrochloride were mixed to the incubated reaction mixture. After 15 min of reaction, diethyl ether was mixed to the same reaction mixture gently and centrifuged at 2000g for 5 min. The absorbance of the colored aqueous phase was recorded at 530 nm. A standard curve was prepared with NaNO<sub>2</sub> and used to calculate the production of O<sub>2</sub><sup>•-</sup>.

For the estimation of H<sub>2</sub>O<sub>2</sub>, leaf and root tissue (40 mg) were extracted with 3 ml of 0.1% (w/v) trichloro acetic acid (TCA) in an ice bath and centrifuged at 10,000g for 15 min.<sup>[16]</sup> The reaction mixture (2 ml) contained tissue extract (0.5 ml), 0.5 ml of 10 mM potassium phosphate buffer (pH 7.0) and 1ml of 1 M KI solution. The absorbance of the mixture was read at 390 nm. Concentration of H<sub>2</sub>O<sub>2</sub> was calculated by using a standard curve prepared with graded solution of H<sub>2</sub>O<sub>2</sub>.

#### ***Determination of lipid peroxidation***

The lipid peroxidation as malondialdehyde (MDA) content was estimated according to the method of Heath and Packer.<sup>[17]</sup> Fresh leaves and root (50 mg) from each sample were

crushed in 2 ml of 5% (w/v) TCA and centrifuged at 10,000g for 10 min at 4°C. Reaction mixture (2.5 ml) contained thiobarbituric acid-TCA solution (2 ml) and tissue extract (0.5 ml) was boiled for 20 min in water bath. After cooling, the absorbance of reaction mixture was recorded at 532 and 600 nm. The values of non-specific absorption at 600 nm were subtracted from the values recorded at 532 nm. The amount of MDA was calculated using the extinction coefficient of  $155 \text{ mM}^{-1} \text{ cm}^{-1}$ .

### ***Total phenolic Contents***

Fresh leaves (50 mg) were extracted with ethanol, and then centrifuged at 10,000g. for 10 min. The aliquots (0.1 mL) were diluted with 1.5 mL of distilled water and 0.1 mL of Folin and Ciocalteu's phenol reagent. After thorough shaking, 0.3 ml sodium carbonate ( $\text{Na}_2\text{CO}_3$ ) (20%) added to the mixtures and the reaction mixtures were then incubated for 30 min in water bath at 40°C. The absorbance of reaction mixtures was recorded at 765nm and compared with standard curve prepared by gallic acid. Total phenolic content is expressed as mg gallic acid equivalents (GAE)  $\text{g}^{-1}\text{FW}$ .<sup>[18]</sup>

### ***DPPH assay***

The measurement of hydrogen donating capability of extract were assessed using DPPH (2, 2' diphenyl-1- picryl hydrazyl) radical as substrate.<sup>[19]</sup> In this assay, 0.05 ml of extract solution was added to 2 ml of 60 mM methanolic DPPH solution and absorbance of each extract were read at 517 nm. The decrease in absorbance at ambient temperature was correlated with the scavenging action of the test compound and compared with gallic acid (used as standard phenolic compound). The radical scavenging activity was calculated using equation-

$$(\text{AC} - \text{AS}) / \text{AC} \times 100$$

AC = Absorbance of Control, AS = Absorbance of Sample solution.

### ***Determination of SOD, POD and GST activities***

For measuring superoxide dismutase (SOD; EC 1.15.1.1) activity , fresh leaf tissues (100 mg) from control and treated seedlings were homogenized in EDTA-phosphate buffer (pH 7.8) and centrifuged at 10,000 g for 20 min at 4°C and supernatant was used as enzyme extract. Reaction mixture (3 ml) contained 50 mM potassium phosphate buffer (pH 7.8), 1.3  $\mu\text{M}$  riboflavin, 0.1 mM EDTA, 13 mM methionine, 63  $\mu\text{M}$  nitro blue tetrazolium (NBT), 0.05 M sodium carbonate (pH 10.2) and enzyme extract (0.1 ml). The reaction mixtures were illuminated for 20 min under white light intensity of  $100 \mu\text{mol photons m}^{-2} \text{ s}^{-1}$ .<sup>[20]</sup> The

photoreduction of NBT (formation of purple formazone) were recorded spectrophotometrically at 560 nm and compared with blank sample having no enzyme extract. One unit (U) of SOD activity is defined as the amount of enzyme required to cause 50 % inhibition in reduction of NBT.

Peroxidase (POD) activity in the leaves of each set of seedlings was determined according to Zhang.<sup>[21]</sup> Fresh leaves (100 mg) were homogenized in 2 ml of 50 mM phosphate buffer (pH 6.1). The homogenate were centrifuged at 10,000g. and the supernatant was used as the crude enzyme extract. Peroxidase activity was measured with guaiacol as the substrate in a total volume of 3 ml. The reaction mixture consisted of 50 mM potassium phosphate buffer (pH 6.1), 1% guaiacol, 0.4% H<sub>2</sub>O<sub>2</sub> and the enzyme extract. Increase in the absorbance due to oxidation of guaiacol was measured at 470 nm at 28°C using extinction coefficient 25.5 mM<sup>-1</sup> cm<sup>-1</sup>. Enzyme activity was calculated in terms of Unit g<sup>-1</sup> FM. One unit of POD activity is the amount of enzyme oxidizing 1 nmol guaiacol min<sup>-1</sup>.

Glutathione-S-transferase (GST) activity was measured following the method of Habig.<sup>[22]</sup> Fresh leaves and root tissues (100 mg) from each sample were homogenized in 100 mM potassium phosphate buffer (pH 6.2) and centrifuged. Enzyme assay was carried out in 2 ml reaction mixtures containing 100 mM potassium phosphate buffer (pH 6.25), 0.75 mM CDNB(1-chloro-2,4-dinitrobenzene), 30 mM GSH (reduced glutathione) and 0.2 ml enzyme extract. The increase in absorbance due to the formation of conjugates between GSH and CDNB were monitored at 340 nm. Enzyme activity was calculated by using an extinction coefficient 9.6 mM<sup>-1</sup> cm<sup>-1</sup>.

## RESULTS AND DISCUSSIONS

The XRD pattern of the functionalized ZnO nanoparticle as synthesized is shown in fig.1. Higher and narrower diffraction peak imply that the ZnO nanoparticles were crystallized well. All the diffraction peaks are in good agreement with the JCPDS file for ZnO (JCPDS 36-1451,  $a=3.249 \text{ \AA}$ ,  $c = 5.206 \text{ \AA}$ ), which can be indexed as the hexagonal wurtzite structure of ZnO. No characteristic peaks of impurities such as Zn (OH)<sub>2</sub> were observed.



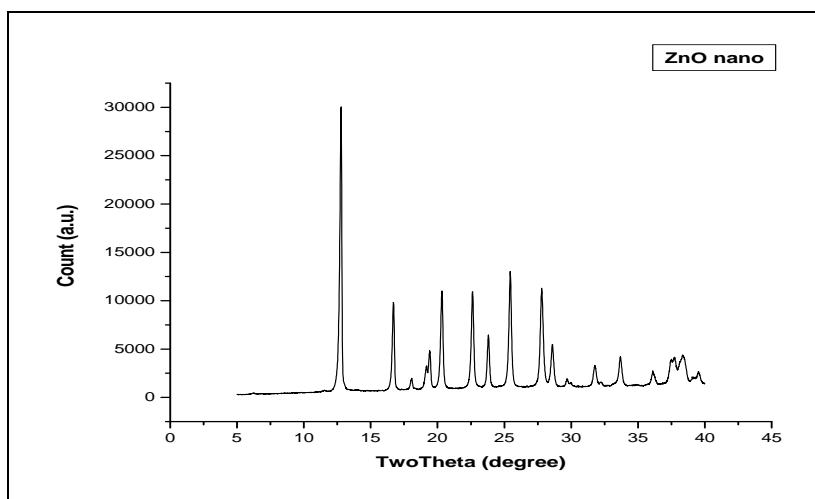


**Fig.1. XRD pattern of the *in situ* functionalized ZnO nanoparticle**

The size of the ZnO nanoparticles was calculated by Debye-Scherrers Equation and was further confirmed by its SEM image (Fig.2). Functionaliation of ZnO was also confirmed by FTIR spectrograph (Fig.3).

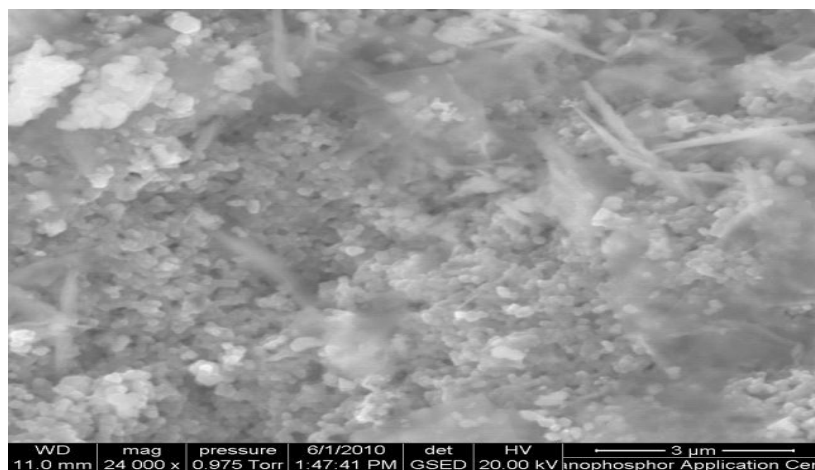


**Fig.2. SEM image of the *in situ* functionalized ZnO nanoparticle**

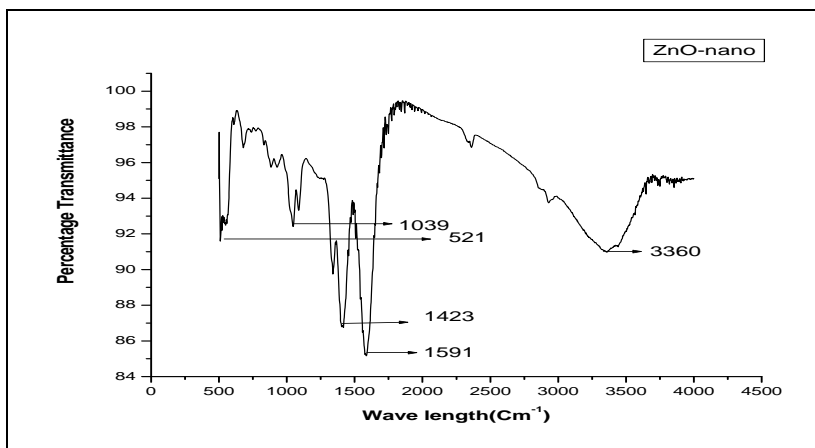


**Fig.3. FTIR of the *in situ* functionalized ZnO nanoparticle**



***Growth and photosynthetic pigments***

A photograph of the growth of all the five case studies is depicted in fig.4. The effect of nano and bulk ZnO can be clearly visualized in this figure. Sapling N<sub>1</sub> with 50 mg/L nano ZnO has shown maximum positive effect with maximum foliage growth. Accordingly, fig.5 shows that there was increase in the fresh weight, root and shoot length in the case of fifth sapling-N<sub>1</sub>, which clearly indicated the maximum positive effect on the plant growth was achieved at this concentration.

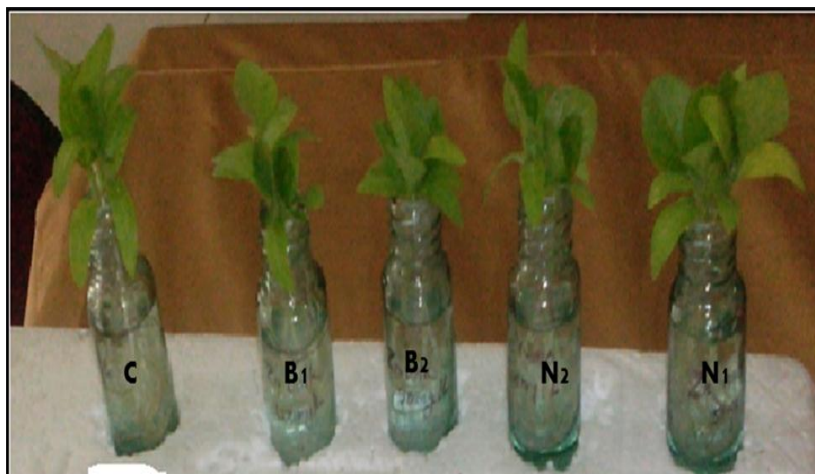


**Fig.4.** The growth behaviour of *Solanum melongena* under the treatment of bulk (B) and nanoparticle (N) of ZnO: C- control (without treatment), B<sub>1</sub>- 50 mg L<sup>-1</sup> bulk ZnO , B<sub>2</sub>- 100 mg L<sup>-1</sup> bulk ZnO , N<sub>1</sub>- 50 mg L<sup>-1</sup> and N<sub>2</sub>- 100 mg L<sup>-1</sup> nano ZnO .

This fact is also supported by the HPLC curves (fig.6) of the extracts. In this figure, the highest peak is observed in the case of N<sub>1</sub> showing that the secretion of indole acetic acid (IAA), an important phytohormone for the promotion of growth, is maximum in this case. [23] It is obvious that when a plant will get sufficient nutrient to promote its growth only then its weight, phytohormone concentration and total soluble protein content (fig.7) will increase i.e. nano ZnO at particular concentration helps in the secretion of growth hormones IAA. [24]

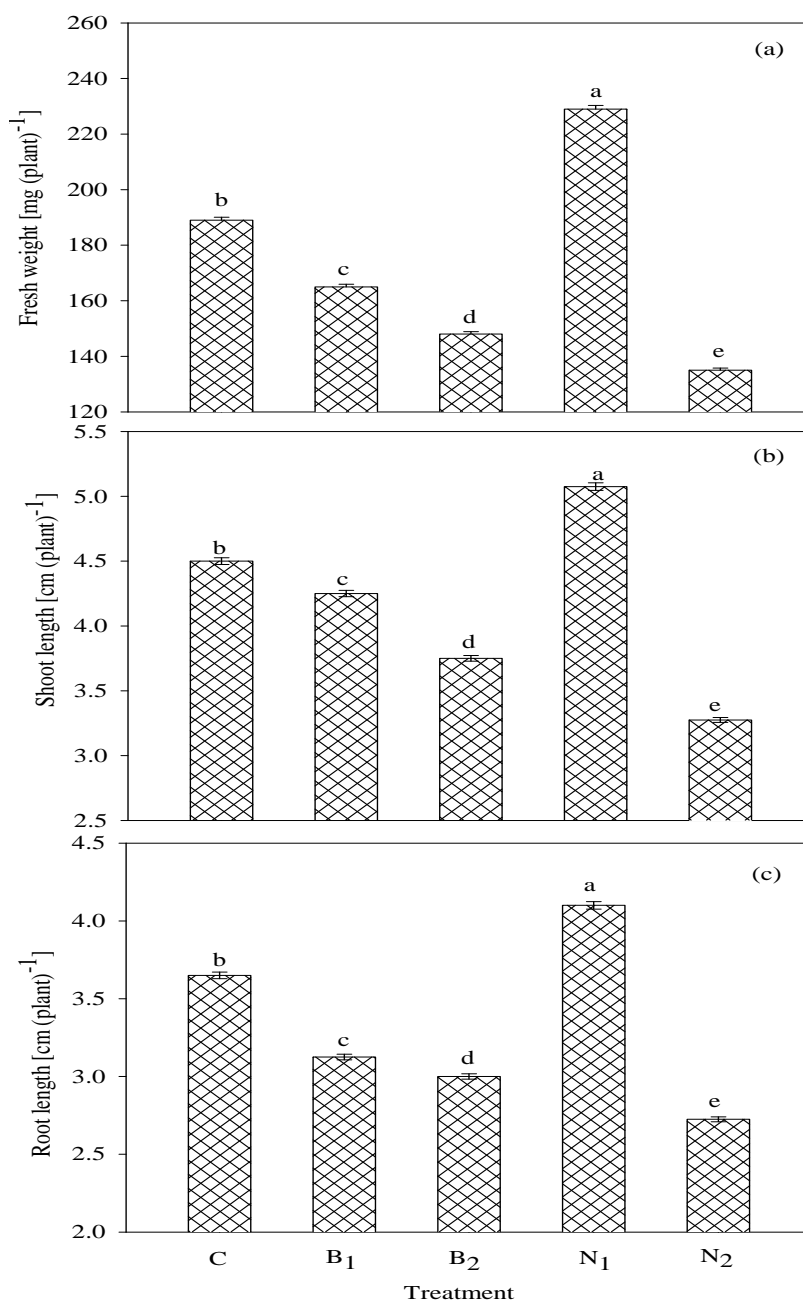


**Fig.5.:** Effect of bulk and nano ZnO on fresh weight (a) shoot length (b) and root length (c) in *Solanum melongena* seedlings. Data are means  $\pm$  standard error of three replicates in each experiments. Bars followed by different letters show significant difference among treatments at  $P<0.05$  significance level according to Duncan's multiple range test.

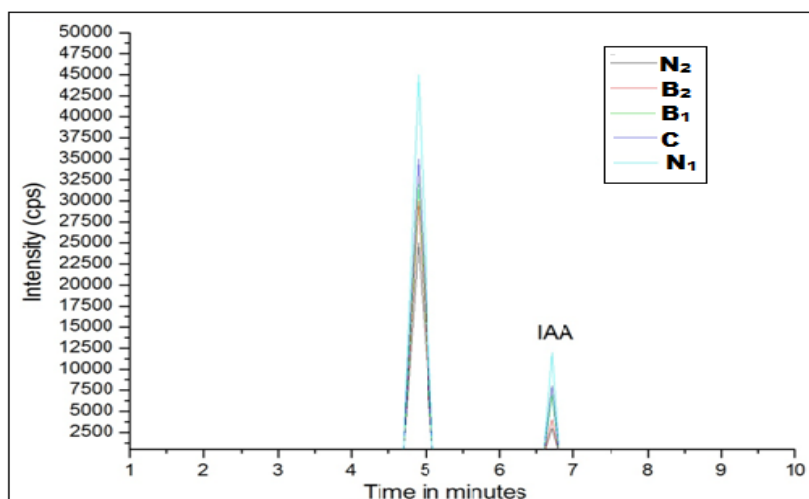


**Fig.6.** HPLC chromatogram showing *in-situ* analysis of IAA in bulk and nano ZnO treated *Solanum melongena* seedlings

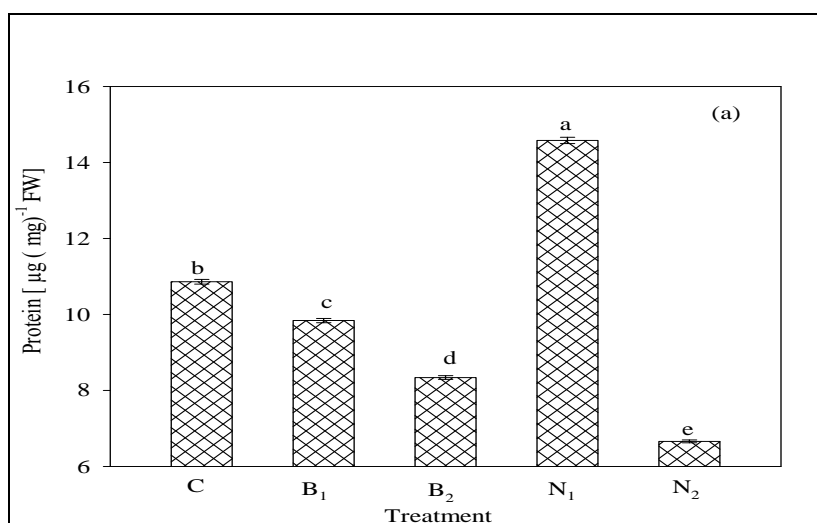


**Fig.7.** Effect of nano and bulk ZnO on total soluble protein content in *Solanum melongena* seedlings. Data are means  $\pm$  standard error of three replicates in each experiments. Bars followed by different letters show significant difference among the treatments at  $P < 0.05$  significance level according to Duncan's multiple range test.

Fig.8. indicates that there was increase in the photosynthetic pigments in N<sub>1</sub> treated seedlings. Higher content of photosynthetic pigments namely, chlorophyll *a*, chlorophyll *b* and carotenoids, would increase the rate of photosynthesis, due to which there was more production of photosynthates, which in turn increased the weight and growth of plant as it was observed in our study.

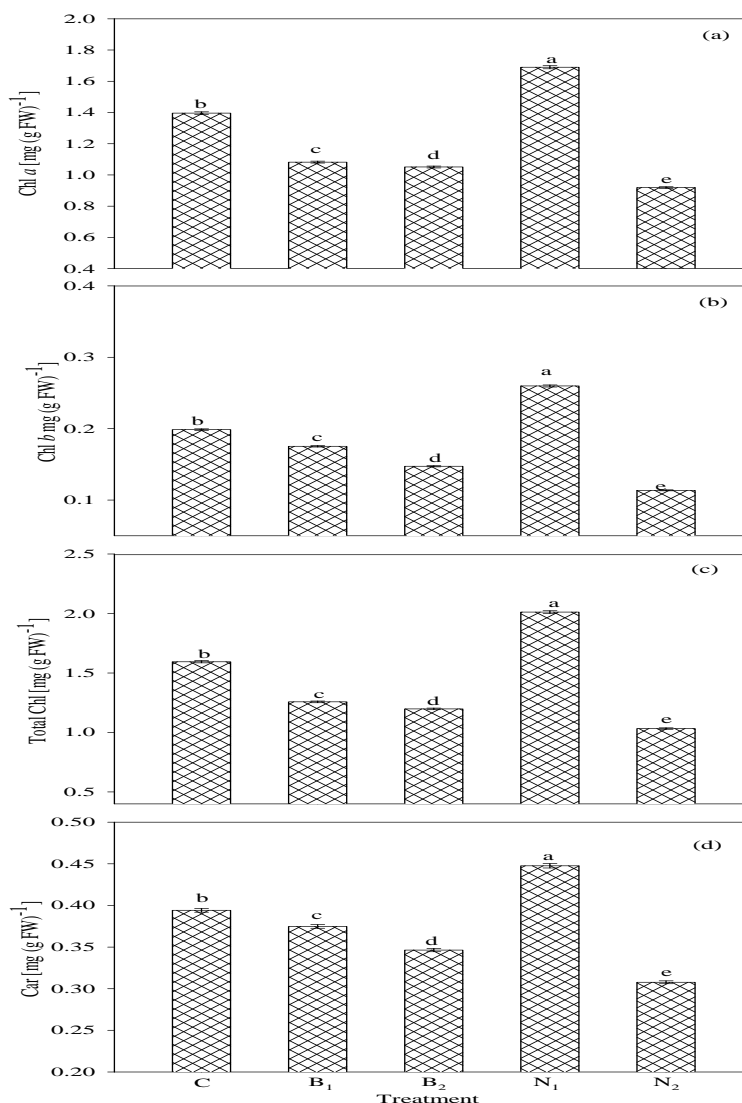


**Fig. 8:** Effect of nano and bulk ZnO on Chl *a* (a), Chl *b* (b), Total Chl (c) and Car contents (d) in *Solanum melongena* seedlings. Data are means  $\pm$  standard error of three replicates in each experiments. Bars followed by different letters show significant difference among the treatments at  $P < 0.05$  significance level according to Duncan's multiple range test.

#### *Superoxide radical, hydrogen peroxide and lipid peroxidation*

Fig.9 shows the effect of bulk and nano ZnO on super oxide radicals (SOR) in test plant extracts. Superoxide radical is considered a major biological source of reactive oxygen species.<sup>[25]</sup> It gives rise to the generation of powerful singlet oxygen ( $^1\text{O}_2$ ) and superoxide ( $\text{O}_2^{\cdot-}$ ) both of which are highly reactive species contribute to oxidative stress. Superoxide may undergo further reduction to produce peroxide ions ( $\text{O}_2^{2-}$ ) and hydrogen peroxide ( $\text{H}_2\text{O}_2$ ). The latter is particularly damaging as a source of highly reactive hydroxyl radicals ( $\cdot\text{OH}$ ) via the Fenton reaction.<sup>[26]</sup> Again, hydroxyl radical is one of the potent reactive oxygen

species in the biological systems. It reacts with polyunsaturated fatty acid moieties of cell membrane phospholipids and causes damage to the cell.<sup>[27]</sup> Fig.9 shows that there was a least production of superoxide free radicals (-5.74 %), H<sub>2</sub>O<sub>2</sub> (-15.38 %) and MDA (-15.6 %) in the case of nano ZnO (N<sub>1</sub>). But nano ZnO (N<sub>2</sub>) has been proven to be toxic having SOR +24%, H<sub>2</sub>O<sub>2</sub> +73 %, and MDA +62.5% as compared to control.

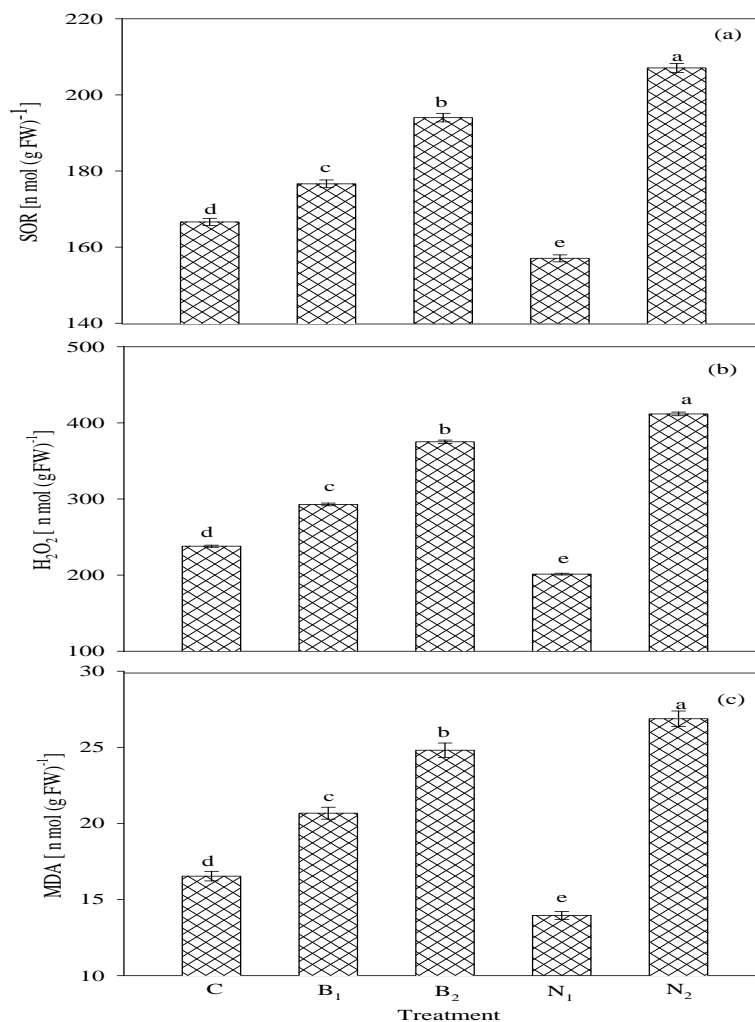


**Fig. 9: Effect of bulk and nano ZnO on production of super oxide radicals (SOR) (a), hydrogen peroxide (H<sub>2</sub>O<sub>2</sub>) (b) and malendehyde (MDA) contents (c) in *Solanum melongena* seedlings. Data are means  $\pm$  standard error of three replicates in each experiments. Bars followed by different letters show significant difference at  $P < 0.05$  significance level according to Duncan's multiple range test.**

It means that at particular concentration only (N<sub>1</sub>) ZnO acts as an oxygen scavenger plays a vital role as an antioxidant. Damage to lipid membranes via lipid peroxidation is one of the most serious effects of ROS, as it not only damages cellular structure and functioning but also results in the propagation of lipid radicals (ROO $\cdot$ ) that may go on to cause further oxidative damage in the cell.<sup>[28]</sup> By scavenging reactive oxygen species (free radicals), ZnO

nanoparticles protect the cells from deleterious effects of oxidative stress caused by the generation of free radicals.<sup>[29]</sup>

**Total phenolic compounds (TPC):** Phenolic contents are important protective components of plant cells. They act as hydrogen donors, reducing agents and quenchers of singlet  $^1\text{O}_2$ . Its synthesis is generally affected in response to different stresses.<sup>[30]</sup> Fig.10 shows that the phenolic contents were also affected significantly due to the increased stress (bulk and nano ZnO). Total phenolic compounds in fractions varied widely, ranging from  $49.9 \pm 4.1$  and  $121.9 \pm 3.1$  mg/g fresh weight expressed as gallic acid equivalents (GAE). The phenolic content was found to be greater in treated seedlings as compared to control. The phenolic content showed increasing trend with increasing concentration of bulk ZnO. Similar trend was also noticed with nano ZnO, however the increment in TPC was minimum in case of  $\text{N}_1$  treated seedlings and maximum in case of  $\text{N}_2$  treatment.

**DPPH assay:** Fig. 10 also showed that among all the fractions tested with various ZnO concentrations, a large decrease in the % DPPH activity in the case of nano ZnO- $\text{N}_1$  (c/f nano ZnO- $\text{N}_2$ ) mixture was observed, which indicates that there was a significant free radical scavenging activity occurred in  $\text{N}_1$  sample under test showing higher inhibition percentage. Results of this study suggest that the extract obtained from the plant grown under nano ZnO- $\text{N}_1$ , though DPPH activity is greater than the control, however, it appears that the amount of antioxidant as compared to the other treatment were less in amount showing that it exhibited less oxidative stress.

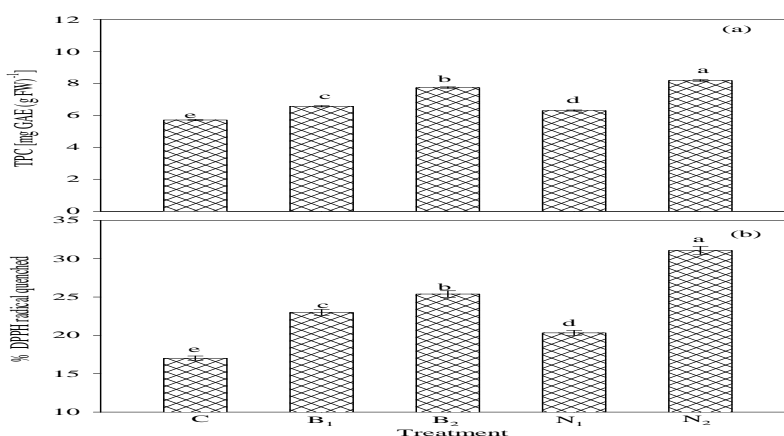


**Fig. 10: Effect of ZnO nano and ZnO bulk on total phenolic content (TPC) (a) and DPPH activity (b) in *Solanum melongena* seedlings. Data are means  $\pm$  standard error of three replicates in each experiments. Bars followed by different letters show significant difference at  $P < 0.05$  significance level according to Duncan's multiple range test.**

### Determination of SOD, POD and GST activities

Superoxide dismutase, catalase, peroxidase and glutathione-S transferase are key enzymes of the antioxidant defense system.<sup>[31]</sup> Fig.11 shows that nano ZnO with increasing concentration ( $N_2$ ) accelerated the formation of active oxygen species, i.e.,  $O_2^-$  and  $H_2O_2$ , in cells progressively causing their damage. POD is capable of eliminating  $H_2O_2$  by oxidizing phenolic compounds at the expense of  $H_2O_2$ . As a consequence of which the activity of superoxide dismutase (SOD) and peroxidase (POD) was enhanced considerably. Lin and Xing have also observed that ZnO nanoparticles and  $Zn^{2+}$  had toxic effects at higher concentrations.<sup>[32]</sup> Increased GST activity can be correlated with the increased concentration and size of the bulk and nano ZnO particles.

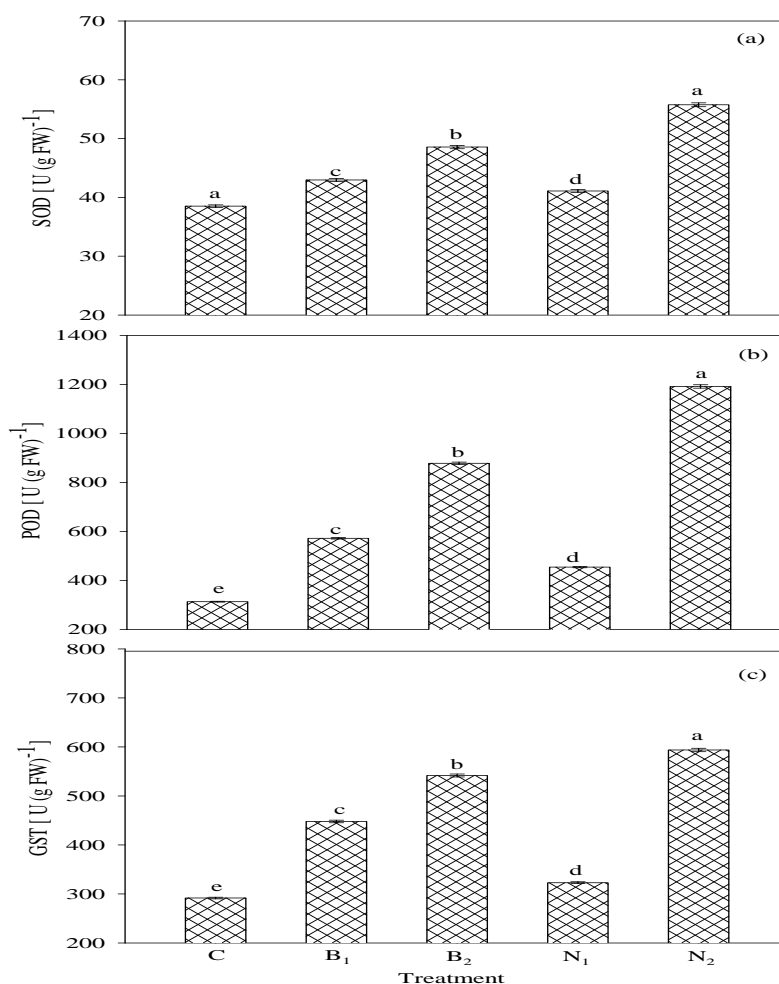


**Fig. 11: Effect of ZnO nano and ZnO bulk on superoxide dismutase (SOD) (a), peroxidase (POD) (b) and glutathione-S-transferase (GST) (c) in *Solanum melongena* seedlings. Data are means  $\pm$  standard error of three replicates in each experiments. Bars followed by different letters show significant difference at  $P < 0.05$  significance level according to Duncan's multiple range test.**



### Mechanism for the adsorption and toxicity of nanoparticles

According to Gupta and Srividya *et al*<sup>[33,34]</sup> adsorptions of nanoparticles occurs through roots by the mechanisms of complexations with functional groups via physical adsorptions and chemical reactions with surface sites, ion exchange and surface precipitations. Lin *et al* have also reported the uptake and translocations of nanoparticles.<sup>[35]</sup> Plant cell wall act as a barrier for easy entry of any external agent including nanoparticles into plant cells. The sieving properties are determined by pore diameter of cell ranging from 5 to 20nm.<sup>[36]</sup> Hence, only nanoparticle with diameter less than the pore diameter of the cell wall could easily pass through and reach the plasma membrane.<sup>[37,38]</sup>

Mechanism of toxicity of nanoparticles is unknown, but release of heavy metal ions, generation of reactive oxygen intermediates (ROIs), and oxidative stress are used to explain the toxicity.<sup>[39]</sup> Toxicity resulting from the high reactive activity of nanoparticles adsorbed on the root surface could not be excluded. Root tips and hairs can secrete large amounts of mucilage, coating the root surface. This mucilage is a highly hydrated polysaccharide, probably a pectic substance, which might contribute to the adsorption of NPs on the root surface.<sup>[40]</sup> The high active reaction occurring on the root-solution interface could make the adsorbed NPs on the root surface dissolved and transported into the root<sup>[41]</sup> Lin and Xing reported that Zn and ZnO NPs affected the growth of radish, rape, and ryegrass, but neither supernatant from centrifugation nor filtrated Zn and ZnO solutions showed significant phytotoxic effects.<sup>[42]</sup>

### Statistical analysis

Results were statistically analyzed by analysis of variance (ANOVA). Duncan's multiple range test was applied for mean separation for significant differences among treatments at  $P < 0.05$  significance level (SPSS 16). The results presented are the means  $\pm$  standard error of three replicates

### CONCLUSION

In conclusion, this study encompasses the synthesis, functionalization characterization and effect of nano as well as bulk ZnO on *Solanum melongena* i.e. brinjal (var. Rajni) plant to investigate its effect on the activity of phytohormones by measuring plant growth and development, photosynthetic pigment in leaves and total soluble proteins. The potent antioxidant activity of functionalized nano ZnO were also determined by determining the level of superoxide radical and hydrogen peroxide, lipid peroxidation, total phenolics, DPPH

assay, SOD, POD and GST activities. It was found that only at particular concentration nano ZnO (50 mg/L) shows its positive response to the plant and at higher concentration of nanoparticles and bulk ZnO show its phytotoxic activity.

### ACKNOWLEDGEMENT

We gratefully acknowledge the financial support provided by University Grants Commission, India [F.No.39-763/2010 (SR)] to carry out this work. We also acknowledge 'Nanotechnology application centre' for helping in literature survey and Prashant Singh for SEM characterization. Authors also want to thank Kumar Kartikeya Yadav of Delhi University for XRD characterization.

### REFERENCES

1. P. Juzenas, W. Chen, Y. P. Sun, M. A. N. Coelho, R. Generalov, N. Generalova, I. L. Christensen, Quantum dots and nanoparticles for photodynamic and radiation therapies of cancer. *Adv. Drug Del. Rev.*, 2008; 60: 1600-1614.
2. X. P. Shen, A. H. Yuan, Y. M. Hu, Y. Jiang, Z. Xu, Z. Hu, Fabrication, characterization and field emission properties of large-scale uniform ZnO nanotube arrays. *Nanotechnology*, 2005; 16: 2039.
3. S.S. Sanjay, A.C. Pandey, P. P. Ankit, M.C. Chattopadhyaya, Fabrication of surfactant sensing membrane with ZnO nano-composite. *Proc. Natl. Acad. Sci. India Sect. A Phys. Sci.*, 2013; 83: 279–85.
4. S.S. Sanjay, R.S. Yadav, A.C. Pandey, Synthesis of lamellar porous photocatalytic nano ZnO with the help of anionic surfactant. *Adv. Mat. Lett.*, 2013; 4: 378-384.
5. X. Gao, L. Yang, J. A. Petros, F. F. Marshall, J. W. Simons, S. Nie, In vivo molecular and cellular imaging with quantum dots. *Curr. Opin. Biotechnol.*, 2005; 16: 63-72.
6. B.Z. Tang, H. Xu, Preparation, alignment and optical properties of soluble poly (phenylacetylene)-wrapped carbon nanotubes. *Macromolecules*, 1999; 32: 2569-2576.
7. P.D. Cozzoli, A. Kornowski, H. Weller, Low-temperature synthesis of soluble and processable organic-capped anatase TiO<sub>2</sub> nanorods. *J. Am. Chem. Soc.*, 2003; 125: 14539- 14548.
8. K. D. Ausman, R. Piner, O. Lourie, R. S. Ruoff, M. Korobov, Organic solvent dispersions of single-walled carbon nanotubes: toward solutions of pristine nanotubes. *J. Phys. Chem. B*, 2000; 104: 8911-8915.

9. G. Kickelbick, U. Schubert, Synthesis, functionalization and surface treatment of nanoparticles. in M I Baraton ed. American Scientific Publishers Stevenson Ranch CA 2003.
10. C. Sanchez, G. D. A. A. Soler-Illia, F. Ribot, T. Lalot, C.R. Mayer, V. Cabuil, Designed hybrid organic–inorganic nanocomposites from functional nanobuilding blocks. *Chem. Mater*, 2001; 13: 3061–3083.
11. S. Yin, Y. Aita, M. Komatsu, J. Wang, Q. Tang, T. Sato, Synthesis of excellent visible-light responsive TiO<sub>2</sub>-xNy photocatalyst by a homogeneous precipitation-solvothermal, *J. Mater. Chem*, 2005; 15: 674-682.
12. H. Å-pik, A.R. Stephen, A.J. Willis, H.E. Street, The physiology of flowering plants (4th ed.). Cambridge University Press, 2005; 191.
13. H.K. Lichtenthaler, Chlorophylls and carotenoids: pigments of photosynthetic biomembranes. *Methods Enzymol*, 1987; 148: 350-382.
14. M.M. Bradford, A rapid and sensitive method for the quantitation of microgram quantities of protein utilizing the principle of protein-dye binding. *Anal. Biochem*, 1976; 72: 248-254.
15. E.F. Elstner, A. Heupel, Inhibition of nitrite formation hydroxyl ammonium chloride: a simple assay for superoxide dismutase. *Anal. Biochem*, 1976; 70: 616-620.
16. V. Velikova, I. Yordanov, A. Edreva, Oxidative stress and some antioxidant systems in acid rain treated bean plants. *Plant Sci*, 2000; 151: 59-66.
17. R.L. Heath, L. Packer, Photoperoxidation in isolated chloroplast. I. Kinetics and stoichiometry of fatty acid peroxidation. *Arch. Biochem. Biophys*, 1968; 125: 189-198.
18. A.L. Waterhouse, Determination of total phenolics. In: Wrolstad RE editor. *Current protocols in food analytical chemistry* (II.1.1-II.1.8). New York: John Wiley & Sons Inc 2001.
19. M.S. Blois, Antioxidant determinations by the use of a stable free radical. *Nature*, 1958; 181: 1199-2000.
20. C.N. Giannopolitis, S.K. Ries, Superoxide dismutase occurrence in higher plants. *Plant Physiol*, 1977; 59: 309-314.
21. X.Z. Zhang, The measurement and mechanism of lipid peroxidation and SOD, POD and CAT activities in biological system. In: X.Z. Zhang, (eds) *Research methodology of crop physiology*. Agriculture Press Beijing, 1992; 208-211.
22. W.H. Habig, M.J. Pabst, W.B. Jakoby, Glutathione-S-transferases, the first enzymatic step in mercapturic acid formation. *J. Biol. Chem*, 1974; 249: 7130-7139.

23. K. Oguchi, N. Tanaka, S. Komatsu, S. Akao, Methylmalonate-semialdehyde dehydrogenase is induced in auxin-stimulated and zinc-stimulated root formation in rice, *Plant Cell Rep*, 2004; 22: 848-858.
24. A.C. Pandey, S.S. Sanjay, R.S. Yadav, Application of ZnO nanoparticles in influencing the growth rate of *Cicer Arietinum*. *J. Exp. Nanoscience*, 2010; 5: 488–497.
25. C. Q. Alves, , J. M. David, J. P. David, M. V. Bahia, R. M. Aguiar, Methods for determination of in vitro antioxidant activity for extracts and organic compounds. *Química Nova*, 2010; 33: 2202-2210.
26. S.S. Gill, N. Tuteja, Reactive oxygen species and antioxidant machinery in abiotic stress tolerance in crop plants. *Plant Physiol. Biochem*, 2010; 48: 909-930.
27. R. A. Khan, M. R. Khan, S. Sahreen, M. Ahmed, Evaluation of phenolic contents and antioxidant activity of various solvent extracts of *Sonchus asper* (L.) Hill. *Chem. Cent. J*, 2012; 6: 12.
28. S. Mano, T. Miwa, S. I. Nishikawa, T. Mimura, M. Nishimura, Seeing is believing: on the use of image databases for visually exploring plant organelle dynamics. *Plant cell physiol*, 2009; 50: 2000-2014.
29. S.S. Sanjay, A.C. Pandey, S. Kumar, A. Pandey, Cell membrane protective efficacy of ZnO nanoparticles, *SOP Trans. Nano-Tech*, 2014; 1: 21-29.
30. C. Rice-Evans, N.J. Miller, G. Paganga, Antioxidant properties of phenolic compounds. *Trends Plant Sci*, 1997; 2: 152-159.
31. A. E. M. M. Afify, H. S. El-Beltagi, A. A. Aly, A. E. El-Ansary, Antioxidant enzyme activities and lipid peroxidation as biomarker for potato tuber stored by two essential oils from Caraway and Clove and its main component carvone and eugenol. *Asian. Pac. J. Trop. Biomed*, 2012; 2: S772-S780.
32. D. Lin, B. Xing, Root uptake and phytotoxicity of ZnO nanoparticles, *Environ. Sci. Technol*, 2008; 42: 5580-5585.
33. V.K. Gupta, A. Rastogi, Biosorption of lead from aqueous solution by green algae *Spirogyra* species: kinetic and equilibrium studies. *J. Hazard. Mater*, 2008; 152: 407- 414.
34. K. Srividya, K. Mohanty, Biosorption of hexavalent chromium from aqueous solutions by *Catla catla* scales: equilibrium and kinetics studies. *Chem. Eng. J*, 2009; 155: 666-673.
35. S. Lin, J. Reppert, Q. Hu, J. S. Hudson, M. L. Reid, T. A. Ratnikova, A. M. Rao, H. Luo, P. C. Ke. Uptake, translocation, and transmission of carbon nanomaterials in rice plants. *Small*, 2009; 5(10): 1128-1132.

36. A. Fleischer, M.A. O'Neill R. Ehwald, The pore size of non-graminaceous plant cell wall is rapidly decreased by borate ester cross-linking of the pectic polysaccharide rhamnogalacturon II. *Plant Physiol*, 1999; 121: 829-38.
37. E. Navarro, A. Baun, R. Behra, N. B. Hartmann, J. Filser, A. Miao, A. Quigg, P. H. Santschi, L. Sigg. Environmental behavior and ecotoxicity of engineered nanoparticles to algae, plants, and fungi. *Ecotoxicol*, 2008; 17: 372-386.
38. M.N. Moore. Do nanoparticles present ecotoxicological risks for the health of the aquatic environment. *Environ. Int*, 2006; 32: 967-976.
39. N. M. Franklin, N. J. Rogers, S. C. Apte, G. E. Batley, G. E. Gadd, P. S. Casey, Comparative toxicity of nanoparticulate ZnO, bulk ZnO, and ZnCl<sub>2</sub> to a freshwater microalga (*Pseudokirchneriella subcapitata*): the importance of particle solubility. *Environ. Sci. Technol*, 2007; 41: 8484-8490.
40. Y. Ma, L. Kuang, X. He, W. Bai, Y. Ding, Z. Zhang, Y. Zhao, Z. Chai, Effects of rare earth oxide nanoparticles on root elongation of plants. *Chemosphere*, 2010; 78: 273-279.
41. A. Manceau, K. L. Nagy, M. A. Marcus, M. Lanson, N. Geoffroy, T. Jacquet, T. Kirpichtchikova, Formation of metallic copper nanoparticles at the soil– root interface. *Environ. Sci. Technol*, 2008; 42: 1766-1772.
42. Lin D, Xing B. Phytotoxicity of nanoparticles: inhibition of seed germination and root growth. *Environ. Pollut*, 2007; 150: 243-50.